The Metallicity of $0.5 < z < 1$ Field Galaxies

C. Marcella Carollo[†]
Columbia University, Department of Astronomy, New York, NY 10027

Simon J. Lilly[†]
University of Toronto, Department of Astronomy, Toronto, ON M5S 3H8 Canada
Herzberg Institute of Astrophysics, Victoria V9E 2E7

[†] Visiting Astronomer at the Canada-France-Hawaii Telescope which is operated by the National Research Council of Canada, the Centre National de la Recherche Scientifique and the University of Hawaii.

Received ______________________; accepted ______________________

ABSTRACT

We have measured the emission line ratios in a sample of 34 CFRS star-forming galaxies with redshifts between $0.5 < z < 1.0$, and computed their metallicities by means of the empirically-calibrated R_{23} metallicity estimator introduced by Pagel et al. (1979). The current analysis concentrates on the 15 galaxies with $L_{H\beta} > 1.2 \times 10^{41}$ erg s^{-1}. Although our results can only be regarded as preliminary until near-IR spectroscopy of Hα and [NII]6583 are available, the metallicities of these galaxies appear to be remarkably similar to those of local galaxies selected in the same way, and there appears to have been little change in the relationship between metallicity and line- and continuum-luminosity from $z \sim 1$ to today. At this stage our results do not support the idea that these galaxies, known to be generally small and with late-type morphologies, are dwarf galaxies brightened by large bursts of star-formation, as had been suggested from previous studies. Rather, our findings are more consistent with a picture in which these systems are the progenitors of today's massive metal-rich galaxies.

subject headings: galaxies: formation - galaxies: evolution - galaxies: metallicity - galaxies: emission lines

1. Introduction

There is now clear evidence from the Canada-France Redshift Survey (CFRS; Lilly et al. 1995a), and other similar surveys, for evolutionary changes in the field galaxy population over the redshift interval $0 < z < 1$ manifested as an increased number of blue galaxies, with rest-frame $(U - V)_{AB} \lesssim 1.4$, and moderate luminosities, $L \sim L^*$. The redshift regime $0.5 < z < 1.0$ appears to be an important epoch in the history of the galaxy population. Evolutionary effects are clearly seen in the galaxy population, and the apparent change of behaviour in the ultraviolet luminosity density of the Universe as a whole around $z \sim 1$ (Lilly et al. 1996; Madau et al. 1996; Steidel et al. 1999) may indicate that this epoch represents a transition between the "high redshift" Universe at $z > 1$ and that seen today. While the large galaxies appear to be absent at $z \sim 2$, large spiral galaxies and early-type galaxies are present at $z \sim 0.8$ in numbers comparable to those seen locally, co-existing with increased numbers of comparably bright but smaller irregular galaxies (Brinchmann et al. 1998, hereafter B98; Lilly et al. 1998; hereafter L98). There is morphological evidence for substantially elevated levels of merger activity at this epoch (Le Fevre et al. 2000).

Much of the work on the $z \sim 1$ field galaxy population has been to date based on gross statistical measures such as the bivariate color-luminosity function (Lilly et al. 1995c; Heyl et al. 1997; Lin et al. 1999). The HST-based studies of the morphologies and sizes of field galaxies in this redshift regime (e.g. B98; L98), and of the internal kinematics of various subsets of these galaxies (Vogt et al. 1997; Guzman et al. 1997; Mallen-Ornelas et al. 1999) have suggested that the most massive galaxies are evolving relatively slowly (Vogt et al. 1997; L98) while the "excess" galaxies in the luminosity function (with $L \sim L^*$ and blue colors) have generally the irregular morphologies (B98), small sizes (3-5 h_{50}^{-1} Mpc, L98) and low velocity dispersions $\sigma < 100$ kms^{-1} (Guzman et al. 1997; Mallen-Ornelas et al. 1999) that are usually associated in the local Universe with galaxies 2-3 magnitudes further down the luminosity function. This suggests at first sight quite a strong luminosity brightening in late-type low mass galaxies.

There are still, however, major gaps in our knowledge of galaxies in the crucial $0.5 < z < 1.0$

redshift regime which make it possible that this interpretation of the morphologies and the kinematic data is incorrect. Not least, the possibility that the small-blue-irregular galaxies are the cores of more massive galaxies —i.e., the "down-sizing" scenario of Cowie et al. (1996)— cannot be ruled out at this stage. For example, the K-band luminosities of typical blue galaxies at $z \sim 0.8$ are comparable to those of today's massive galaxies, leading to suggestions that at least some of these blue objects may be indeed the progenitors of massive systems.

There has hitherto been almost no systematic study in the $0.5 < z < 1$ regime of the physical diagnostics that are familiar from studies of the local Universe. For local galaxies, combinations of strong emission lines are routinely used to determine or constrain the nature of the ionizing radiation (Veilleux & Osterbrock 1987), the amount of reddening, and the metallicity of the interstellar medium (ISM; Pagel et al. 1979; Kennicutt 1998; Stiavelli 1998; Kobulnicky et al. 1999). Although a rigorous determination of the ISM metallicity requires knowledge of electron temperature derivable only from intrinsically weak lines, diagnostic line ratios based on stronger lines have been empirically calibrated. In particular, the R_{23} parameter, $R_{23} = ([OII]3727 + [OIII]4959 + 5007)/H\beta$ (Pagel et al. 1979), has been empirically calibrated against metallicity, with an intrinsic scatter of only 0.2 dex. It is a weak function of the ionization ratio [OIII]4959+5007/[OII]3727. A reversal in R_{23} occurs at $Z \sim 0.3 Z_{\odot}$ due to cooling effects, so a low- and a high-metallicity solution are associated with most values of R_{23}. This degeneracy can however be broken using the [OIII]5007/[NII]6584 ratio (Kobulnicky et al. 1999). Based on data on relatively low redshift galaxies, Kobulnicky et al. have discussed in detail the potential accuracy that could be obtained in using R_{23} to measure metallicities of unresolved galaxies at high redshifts. These authors examined theoretically the effects of dust reddening, of $H\beta$ absorption, of spatial averaging over extended galaxies with abundance gradients, and the possible effects of diffuse interstellar gas, and provided prescriptions for dealing with these effects.

Determining the metallicity of the ISM of distant starforming field galaxies is of particular importance, both as a general indicator of the evolutionary state of these systems, and as a constraint on their possible present-day descendants. Some work has been done to determine the metal content of galaxies at redshifts of about $0.1 < z < 0.5$ (Kobulnicky & Zaritsky 1999); no information has however been available about the ISM metallicities of galaxies in the $0.5 < z < 1.0$ redshift interval. We have therefore begun a program of systematic emission line spectroscopy of CFRS galaxies to determine the ISM metallicity of $0.5 < z < 1.0$ field galaxies, and to study how the metal content in these systems correlates with galaxy luminosity, star-formation rate, structure and morphology. Our program uses the R_{23} metallicity estimator and therefore requires spectroscopy of the [OII]3727, [OIII]4959,5007 and Hβ lines, which in this redshift range are shifted into the 5000 $\AA$ - 1 μm wavelength region. Supplementary spectroscopy of Hα, [NII]6584 and [SII]6717,6731 lines, which are shifted into the near-infrared J-band, allows determination of the reddening, isolation of active galactic nuclei, and the breaking of the R_{23}-degeneracy with metallicity.

In this Letter we report the first results of our program which are based on deep multi-object spectrophotometry over the $0.5 < \lambda < 1.0\mu$m range. Infrared spectrophotometry has already been acquired for one object, and will be obtained in due course for the remaining galaxies, but the optical data on its own already provides a set of homogeneous data that can immediately be compared at a phenomenological level with the equivalent local sample (see e.g. Jansen et al. 2000). Throughout this paper we use $H_o = 50$ Mpc/Km/s and $q_o = 0.5$, and refer to solar metallicity $Z_\odot$ as $12 + Log(O/H) = 8.9$.

2. Sample Selection, Observations and Data Reduction

The observations were carried out on the nights 5-7 March 2000 at the 3.6m Canada-France-Hawaii Telescope (CFHT) using the MOS spectrograph (Le Fevre et al. 1994) with the STIS-2 CCD detector with 21 μm pixels. A red-blazed grating with 300 l/mm and a short-wavelength cutoff filter yielded spectra between 5000$\AA$ and 1 μm and about 20 objects were observed on each multi-slit mask with slits $20''$ long and $1.3''$ wide, giving a spectral resolution of $R \sim 600$. One mask was observed in each of the CFRS-10 and CFRS-14 fields (Le Fevre et al. 1995; Lilly et al.

1995b).

Spectroscopy at $\lambda \geq 7600\AA$ is challenging on account of the OH forest. The most important factors that hamper accurate spectroscopic measurements are sky-subtraction and fringe removal. The use of relatively long slitlets ($\sim 20''$) and nine 2700s exposures allowed us to offset the target galaxies along the slit at each integration, and thus to largely eliminate defects in the sky-subtraction that are fixed relative to the chip (e.g. those arising from chip fringing, imperfections in the slit profile, and distortions introduced by the spectrograph camera). The spectra were reduced with standard IRAF routines and calibrated via observations of two spectrophotometric standards. The spectra were corrected for (small) airmass effects but not for Galactic reddening, since this is small ($E_{B-V} < 0.03$, Burstein & Heiles 1984). Comparisons of the spectra of standard stars observed through different slits in the masks indicated that the relative spectrophotometric calibration over the wavelength range of interest was about 10% (r.m.s.). However, the uncertainties in the relative line flux measurements were usually dominated by systematic uncertainties in establishing the local continuum, and these were conservatively estimated by exploring rather extreme possibilities. The errors in the line ratios were derived from adding in quadrature these two sources of uncertainty. In several cases, the strength of the [OIII]4959 line was only poorly estimated and in these cases the strength of this line was assumed to be 2.85 times that of [OIII]5007. In a few cases, the Hβ and/or [OIII]5007 lines were not convincingly seen in the spectra; for these galaxies, conservative upper limits were estimated through comparison with nearby features in the spectra that were known to be unreal.

The 34 target galaxies were selected from the CFRS to have, in addition to the original $I_{AB} < 22.5$ photometric selection, an [OII]3727 flux in excess of 7×10^{-17} erg s^{-1}cm^{-2} in order to ensure strong enough lines for a measurement of the R_{23} parameter. The observational noise in the R_{23} measurement is usually dominated by the uncertainty in the strength of Hβ which appears in the denominator of R_{23}. The Hβ luminosity is likely to be closely related to the star-formation rate and represents an astrophysically useful reference to galaxies in the local Universe. Unfortunately, Hβ measurements were not available beforehand for most of the target galaxies because of the long wavelength cut-off (at about 8400 $\AA$) of the original CFRS spectra. A close approximation to an $H\beta$-luminosity selected sample can only be constructed a posteriori. The analysis presented in this paper is based on the 15 objects —about 50% of the original [OII]3727 selected sample observed during the run— with Hβ luminosities above $L_{H\beta} > 1.2 \times 10^{41}$ erg s^{-1}. It should be noted that any objects missing from such a sample would have low [OII]3727/Hβ ratios, and thus generally low R_{23} values which generally correspond to high metallicities. This high-$L_{H\beta}$ selection well samples the 'blue' CFRS galaxy population with restframe $(U - V)_{AB} \lesssim 1.4$ (Table 1). Two of the highest redshift galaxies, at redshifts $z = 0.8718$ and 0.9203, respectively, have easily detectable [NeIII]3869. On the $Log([NeIII]3869/H\beta)$ versus $Log([OII]3727/H\beta)$ plane of Rola et al. (1997), these systems (unlike the other 13) occupy locations typical of the local AGN population. Therefore, although they are formally part of our high-$L_{H\beta}$ sample, these probable-AGN will be distinguished in our comparison with the local galaxies. The remaining 13 high-$L_{H\beta}$ objects span the redshift range $0.6 < z < 1$ with a median redshift $z \sim 0.783$.

Three high redshift galaxies in the original sample of 34 had upper limits to their Hβ luminosities which were above our $L_{H\beta} = 1.2 \times 10^{41}$ erg s^{-1} threshold, possibly putting these systems into the high-$L_{H\beta}$ sub-sample that is discussed in this paper. The line ratios for these galaxies are necessarily uncertain; however, we have included these systems in the figures for completeness, and assigned to them the range of line ratios that they would have if their Hβ luminosities were indeed above our threshold. We have however identified these three objects with different symbols, as a reminder that they may actually not belong to the high-$L_{H\beta}$ sub-sample.

We report in Table 1 the relevant parameters for the 15 $L_{H\beta} > 1.2 \times 10^{41}$ erg s^{-1} galaxies and for the three galaxies with upper limits on $L_{H\beta}$ above this threshold.

3. Results and Discussion

Figures 1a and 1b show the [OIII]5007/[OII]3727 versus R_{23} relation for the local field sample of Jansen et al. (2000) and the high-$L_{H\beta}$ CFRS galaxies of our sample, respectively. The galaxies of the Jansen et al. sample were selected from the CfA redshift catalog (Huchra et al. 1983) to span a large range in absolute B magnitude (from -14 to -22), while sampling fairly the changing mix of morphological types as a function of luminosity. In the figures, the solid and dashed lines are lines of constant metallicity. From left to right, the dashed lines indicate increasing metallicities from $0.02Z_{\odot}$ to $0.2Z_{\odot}$. At $Z \sim 0.3Z_{\odot}$, the reversal of R_{23} occurs, and the curves of constant metallicity then follow the solid-line sequence in which Z rises up to about $3Z_{\odot}$ from right back to left. The $Z = Z_{\odot}$ curve is highlighted with a thicker linewidth. In order to appropriately compare the local and the high–z samples, the local Jansen et al. galaxies which have $\mathrm{L}_{H\beta} > 1.2 \times 10^{41}$ ergs s^{-1} are identified with large circles; local galaxies with smaller $H\beta$ luminosities are represented by small circles. Furthermore, in Fig 1a, filled symbols represent objects which have a flux ratio $[OIII]5007/[NII]6584 > 2$ and thus metallicities $Z \lesssim 0.5Z_{\odot}$, and empty symbols indicate objects with higher metallicities, as indicated by a flux ratio $[OIII]5007/[NII]6584 < 2$ (see Edmunds & Pagel 1984). In Figure 1b, the high–z galaxies are represented by the filled squares, with the exception of the two probable-AGN (identified by the asterisks), and of the three objects which may or may not be in the sample on account of their Hβ upper limits (empty squares). The fiducial dotted-line box in both panels encompasses the bulk of the Jansen's galaxies. The arrows on the right-side of the figures represent the direction in which the points of the diagram would shift due to reddening by dust (as described by Cardelli et al. 1989); the length of the arrows refer to an $E(B - V) = 0.3$ magnitudes at $z = 0.7$. The effects of reddening are a function of the [OIII]5007/[OII]3727 ratio.

Several things are apparent in Figures 1a and 1b. First, the high redshift galaxies fall in the R_{23} versus [OIII]/[OII] plane in locations that are occupied by galaxies in the local Jansen et al. (2000) sample. Furthermore, once the AGNs are excluded, the high redshift sample selected to have $L_{H\beta} > 1.2 \times 10^{41}$ erg s^{-1} occupies the same restricted location in the R_{23} versus [OIII]/[OII] plane as do the objects in the local Universe with similarly high $H\beta$ luminosities. At both epochs, galaxies selected to have the same Hβ luminosities exhibit the same range of R_{23} and [OIII]/[OII]. (We note that there may possibly be a small displacement of the high redshift galaxies towards the upper edge of the dotted box in Figure 1a. This could conceivably be due to the effects of higher dust extinction at high redshifts; it would be premature to claim this at this stage.)

It is also apparent on Figure 1b that once the two probable-AGNs are again excluded, there are no high-$L_{H\beta}$ objects at high redshifts (at least in this still small sample) that have $R_{23} \sim 7$, the value that is non-degeneratively associated with intermediate metallicities, i.e. $Z \sim 0.3 Z_{\odot}$. The Z-degenerate R_{23} values that are measured for the high-z, high-$L_{H\beta}$ galaxies indicate either rather low ($\lesssim 0.1 Z_{\odot}$) or rather high ($\sim Z_{\odot}$) metallicities for these systems. This is again similar to what is observed in the local sample: high-$L_{H\beta}$ galaxies avoid the intermediate metallicity regime both at the present and at the $z \sim 1$ epoch.

The similarity between the high and low redshift samples is further illustrated in Figure 2, which shows the relationship between R_{23} and continuum luminosity M_B. There is a rather startling similarity between the high-z and the local galaxies on this diagram. There is little evidence for an evolutionary change in the relationship between metallicity (as estimated from R_{23}) and the line and continuum luminosities for high-$L_{H\beta}$ field galaxies between $z \sim 0$ and $z \sim 0.8$. This extends to higher redshifts the findings of Kobulnicky & Zaritsky (1999) which was based on a similar sample at $0.1 < z < 0.5$.

For one of the non-AGN galaxies, CFRS-14.0393, we have already obtained a Keck spectrum in the J-band, and analysed it to derive the intensity of the [NII]6584 emission line. We will report the details on this analysis elsewhere. The important fact, relevant for the current discussion, is that the [OIII]5007/[NII]6584 ratio that this J-band spectrum has allowed us to measure for this ($z = 0.6035$) object undoubtedly places it on the high-metallicity branch of the R_{23} parameter, with a metallicity quite close to the solar value. This one case argues in favour of a high, i.e. about solar metallicity for at least some objects in our $0.5 < z < 1$ high-$L_{H\beta}$ sample. The HST morphology of this object is that of a regular two-armed spiral (Schade et al. 1995), and so it is possibly not surprising that this galaxy has a high metallicity. It may be that our high-$L_{H\beta}$ selection favours large well-formed galaxies relative to the general blue CFRS population. However, there is no indication that this is the case from the HST morphology of three additional objects for which the HST data are available (CFRS-10.1213, CFRS-14.0972 and CFRS-14.1258).

Of course, until we obtain the infrared spectroscopy for the entire sample, the R_{23} degeneracy with Z does not allow us to prove on what branch —i.e., the low- or the high-metallicity one— each individual high-z galaxy lies, and the possibility remains that some objects have indeed metallicities $Z \lesssim 0.1 Z_\odot$. However, at this stage, the absence of any galaxies with $Z \sim 0.3 Z_\odot$ makes this possibility rather contrived, since it would imply a bimodal distribution of metallicities with a "gap" around such intermediate values of Z. Therefore, although confirmation must await the infrared spectroscopy, the best working hypothesis seems the one where *all* of the analysed high-$L_{H\beta}$ high redshift galaxies have relatively high metallicities, i.e. within 40% of solar.

The consequences of these findings are interesting in the context of the studies of sizes, morphologies and kinematics of high-redshift galaxies discussed above. It is clear in fact that, at this stage, the metallicity measurements of $0.5 < z < 1$ systems do not support the idea that many of the small and irregular blue L* galaxies that are responsible for the evolution of the luminosity function back to $z \sim 0.8$, and which dominate the CFRS at these redshifts (B98; L98) are low mass (i.e. low metallicity) dwarfs brightened by substantial luminosity evolution. In contrast, the metallicity data seem to suggest the interesting possibility that these small irregular galaxies are in fact the progenitors of today's massive, metal-rich galaxies, but seen in an earlier phase of their evolution when they were already significantly metal-rich but morphologically more disturbed and smaller. Although about a 1/3 of the CFRS has been imaged by HST (see Schade et al 1996; B98), the overlap with this spectroscopic sample is as yet still small. Testing this idea by studying the morphologies of these metal-rich systems will have important consequences for our understanding of the evolutionary path of massive galaxies.

We thank Marijn Franx, Jules Halpern, Nino Panagia and Massimo Stiavelli for helpful discussions. SJL's research in Toronto is supported by the Natural Sciences and Engineering Research Council of Canada and by the Canadian Institute for Advanced Research, and this support is gratefully acknowledged.

REFERENCES

Brinchmann et al. 1998, ApJ, 499, 112 (B98)

Burstein, D., Heiles, C., 1982, AJ, 87, 1165

Cardelli, J. A., Clayton, G. C., Mathis, J.S., 1989, ApJ, 345, 245

Cowie, L., et al. 1996, AJ, 112, 839

Edmunds, M.G., Pagel, B.E.J., 1984, MNRAS, 211, 507

Guzman et al. 1997, ApJ, 489, 559

Heyl, J., et al. 1997, MNRAS, 285, 613

Huchra, J.P., Davis, M., Latham, D., Tonry, J., 1983, ApJS, 52, 89

Jansen, R.A., Fabricant, D. Franx, M. Caldwell, N., 2000, ApJS, 126, 331

Kennicutt, R., 1998, in "The NGST", ESA, p.81

Kobulnicky et al. 1999, ApJ, 514, 544

Kobulnicky & Zaritzky, 1999, ApJ, 511, 118

Le Fevre, O., Crampton, D., Felenbok, P., Monnet, G., 1994, A&A, 282, 325

Lilly, S.J., et al. 1995a, ApJ, 455, 50

Lilly, S.J., et al. 1995b, ApJ, 455, 75

Lilly, S.J., et al. 1995c, ApJ, 455, 108

Lilly, S.J., et al. 1996, ApJL, 460, 1

Lilly et al. 1998, ApJ, 500, 75 (L98)

Lilly, S.J., Carollo, C.M. & Mallen-Ornelas, G., 2000, in preparation

Lin, H., et al. 1999, ApJ, 518, 533

Le Fevre, O., et al. 2000, MNRAS, 311, 565

Madau, P., et al. 1996, MNRAS, 283, 1388

Mallen-Ornelas, G., et al. 1999, ApJL, 518, 83

Pagel, B.E.J., Edmunds, M.G., Blackwell, D. E., Chun, M.S., Smith, G., 1979, MNRAS, 189, 95

Schade, D., Lilly, S.J,; Crampton, D., Hammer, F., Le Fevre, O., Tresse, L., 1995, ApJ, 451, L1

Steidel, C., et al. 1999, ApJ, 519, 1

Stiavelli, M., 1998, in “The NGST”, ESA, p.71

Veilleux & Osterbrock 1987, ApJS, 63, 295

Vogt, N., et al. 1997, ApJL, 479, 121

This manuscript was prepared with the AAS LaTeX macros v3.0.

Fig. 1.— The [OIII]5007/[OII]3727 versus R_{23} relation for the local field sample of Jansen et al. (Panel a) and the $\mathrm{L}_{H\beta} > 1.2 \times 10^{41}$ ergs s^{-1} CFRS galaxies of our sample (Panel b). Symbols are explained in the text. The $0.5 < z < 1$ galaxies with $\mathrm{L}_{H\beta} > 1.2 \times 10^{41}$ ergs s^{-1} appear to have metallicities as high as the equivalent high-$L_{H\beta}$ objects in the local universe.

Fig. 2.— The R_{23} versus absolute B magnitude relation for the galaxies in the local universe (circles) and those in the $0.5 < z < 1$ redshift regime (squares and asterisks). Symbols are as in Figures 1a and 1b, and are explained in the text. Above the $\mathrm{L}_{H\beta} > 1.2 \times 10^{41}$ ergs s^{-1} cutoff, the distribution of points for the local and the high-z galaxy populations is identical.

CFRS-#	M_B (mag)	z	$(V-I)_{obs}$	$(U-V)_{rest}$	Log(R_{23})	Log([OIII]5007/[OII]3727)
10.0498†	-21.22	0.920	0.66	0.41	1.38 (-0.5)	0.20 (0.03)
10.1213	-20.94	0.815	1.27	0.97	0.47 (-0.29 / +0.38)	-0.19 (-0.31 / +0.19)
10.1925	-21.00	0.783	1.00	0.62	0.51 (0.12)	-0.13 (-0.19 / +0.14)
(10.2164)	-22.64	0.859	2.95	2.48	0.08 (-0.5)	-1.20 (-1.45)
(10.2183)	-21.87	0.910	1.47	1.15	0.56 (-0.5)	-1.15 (-1.04)
10.2418	-22.00	0.796	2.39	2.01	0.19 (-0.27 / +0.24)	-1.10 (-0.80)
10.2428†	-21.23	0.872	1.78	1.30	0.83 (0.07)	0.16 (0.01)
14.0217	-20.94	0.721	1.00	0.64	0.56 (-0.09 / +0.10	-0.17 (0.04)
14.0272	-21.98	0.670	1.19	0.92	0.09 (-0.25 / +0.29)	-1.25 (-0.76)
14.0393††	-21.85	0.603	0.98	0.72	0.45 (-0.11 / +0.12)	-0.28 (0.03)
14.0438	-22.12	0.988	0.74	0.51	0.47 (0.10)	-0.75 (-0.13 / +0.10)
(14.0497)	-21.22	0.800	1.10	0.73	0.19 (-0.14)	-1.30 (-1.44)
14.0538	-21.18	0.677	0.57	0.20	0.70 (0.07)	-0.08 (0.02)
14.0605	-20.69	0.837	0.40	0.10	0.62 (0.09)	0.22 (0.03)
14.0818	-22.27	0.901	1.12	0.83	0.47 (0.17)	-0.22 (-0.31 / +0.18)
14.0972	-21.37	0.810	0.82	0.43	0.62 (0.05)	0.02 (0.02)
14.1258	-20.14	0.647	0.97	0.65	0.54 (0.07)	0.06 (0.02)
14.1386	-21.46	0.744	1.05	0.69	0.25 (-0.14 / +0.15)	-0.40 (-0.06 / +0.05)

Table 1: The 15 galaxies with $L_{H\beta} > 1.2 \times 10^{41}$ erg s^{-1}, and the three additional objects with $L_{H\beta}$ upper limits above this threshold. These three objects are identified by a parenthesis in column 1, which lists the CFRS identification number (Lilly et al. 1995b; Le Fevre et al. 1995). The remaining columns list, respectively, the absolute B magnitude, the redshift, the observed $V-I$ and the rest-frame $U-V$ colors (AB magnitudes; from Lilly et al. 1995c), the R_{23} parameter and the [OIII]5007/[OII]3727 ratio. In colum 1, the symbol "†" identifies the two probable-AGN; the "††" identifies the one galaxy with the available J-band Keck spectrum. In the last two columns, the positive numbers in parenthesis are the error bars on the reported measurements (single-valued entries refer to symmetric errors); negative numbers in parenthesis indicate that the reported values are limits (lower ones for [OIII]5007/[OII]3727, upper ones for R_{23}).

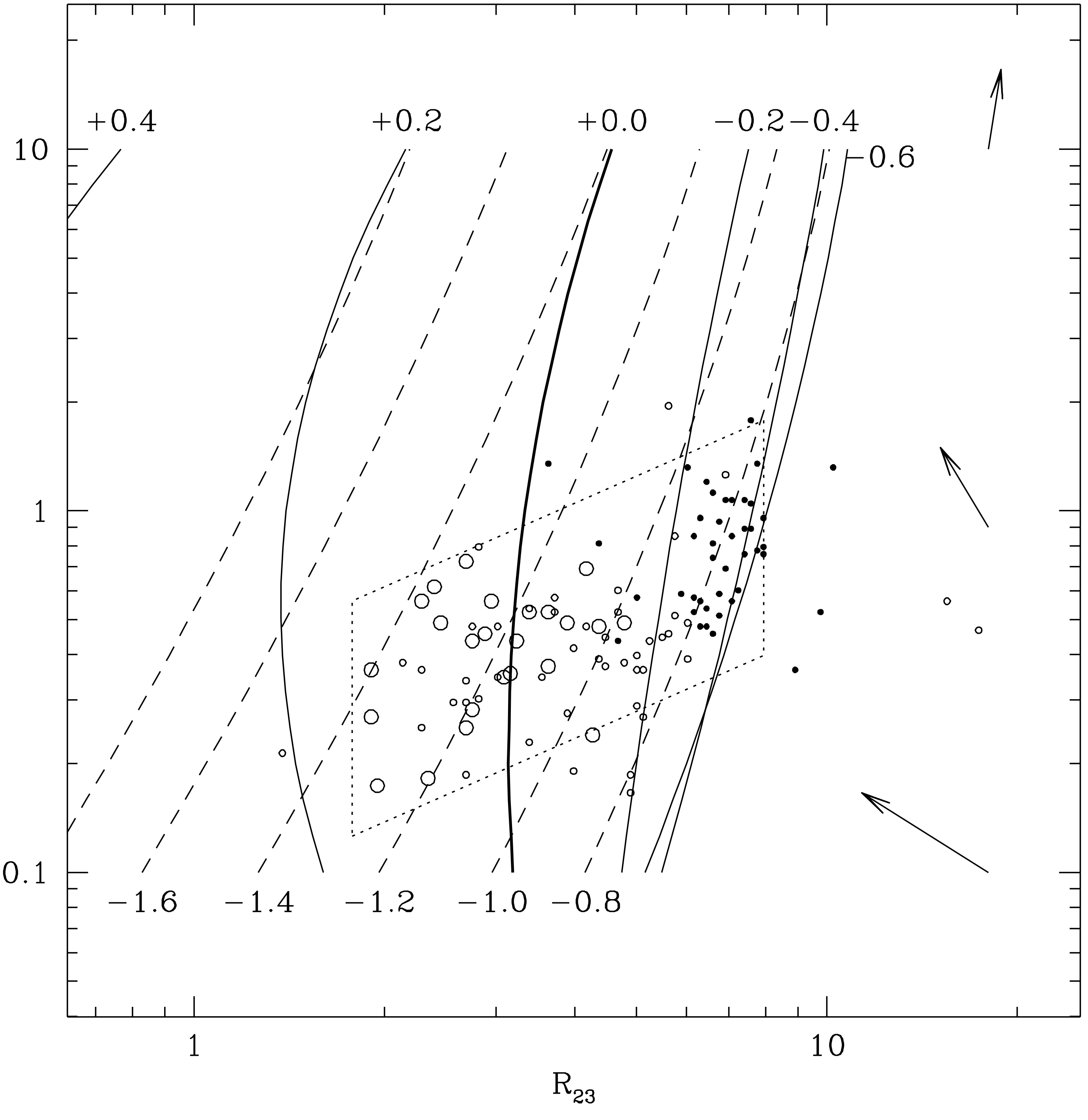

+0.4
+0.2
+0.0
−0.2
−0.4
−0.6
−1.6
−1.4
−1.2
−1.0
−0.8
10
1
0.1
OIII/OII
1
10
R$_{23}$

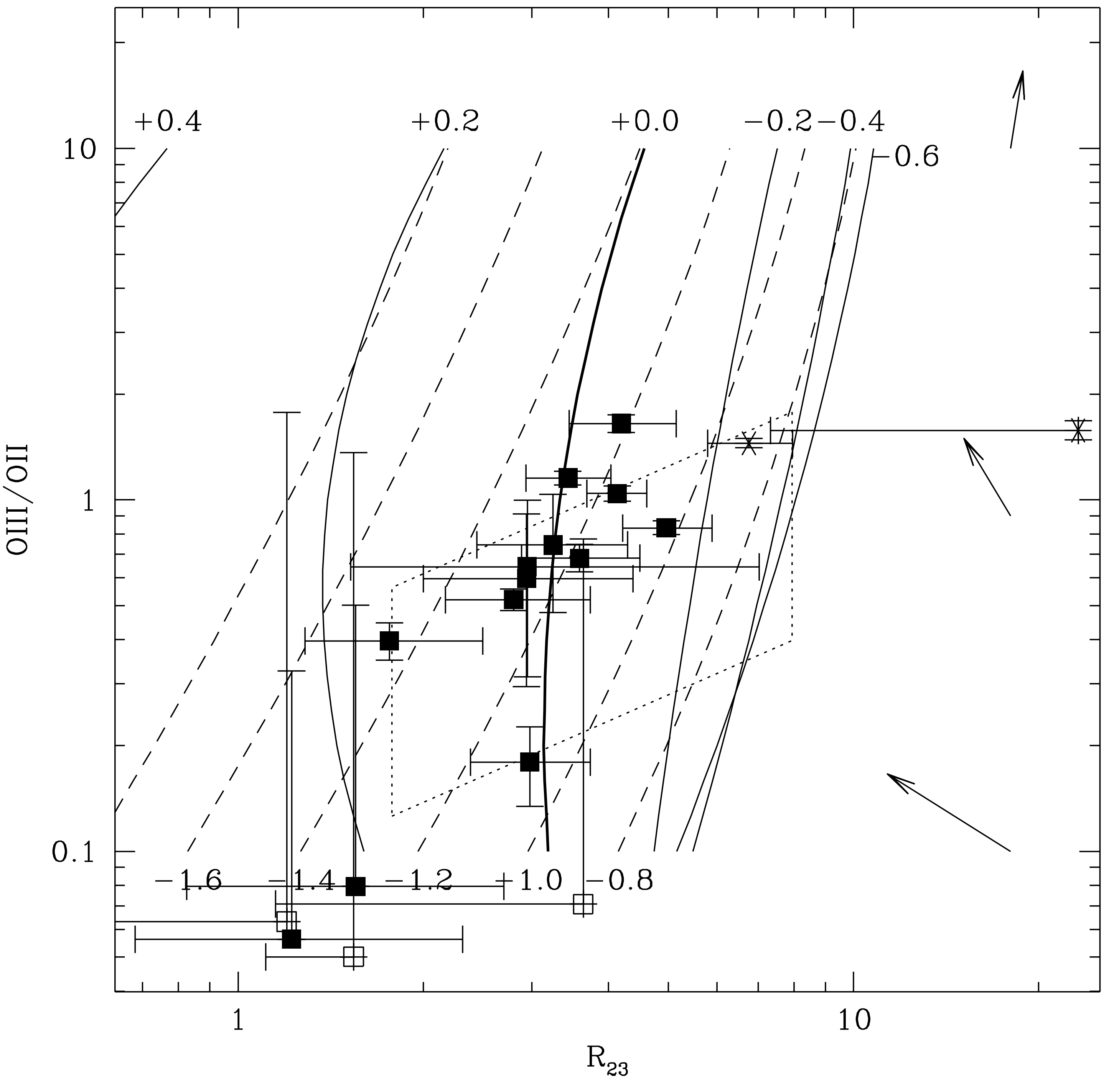
+0.4
+0.2
+0.0
−0.2
−0.4
−0.6
−1.6
−1.4
−1.2
−1.0
−0.8
10
1
0.1
OIII/OII
1
10
R$_{23}$

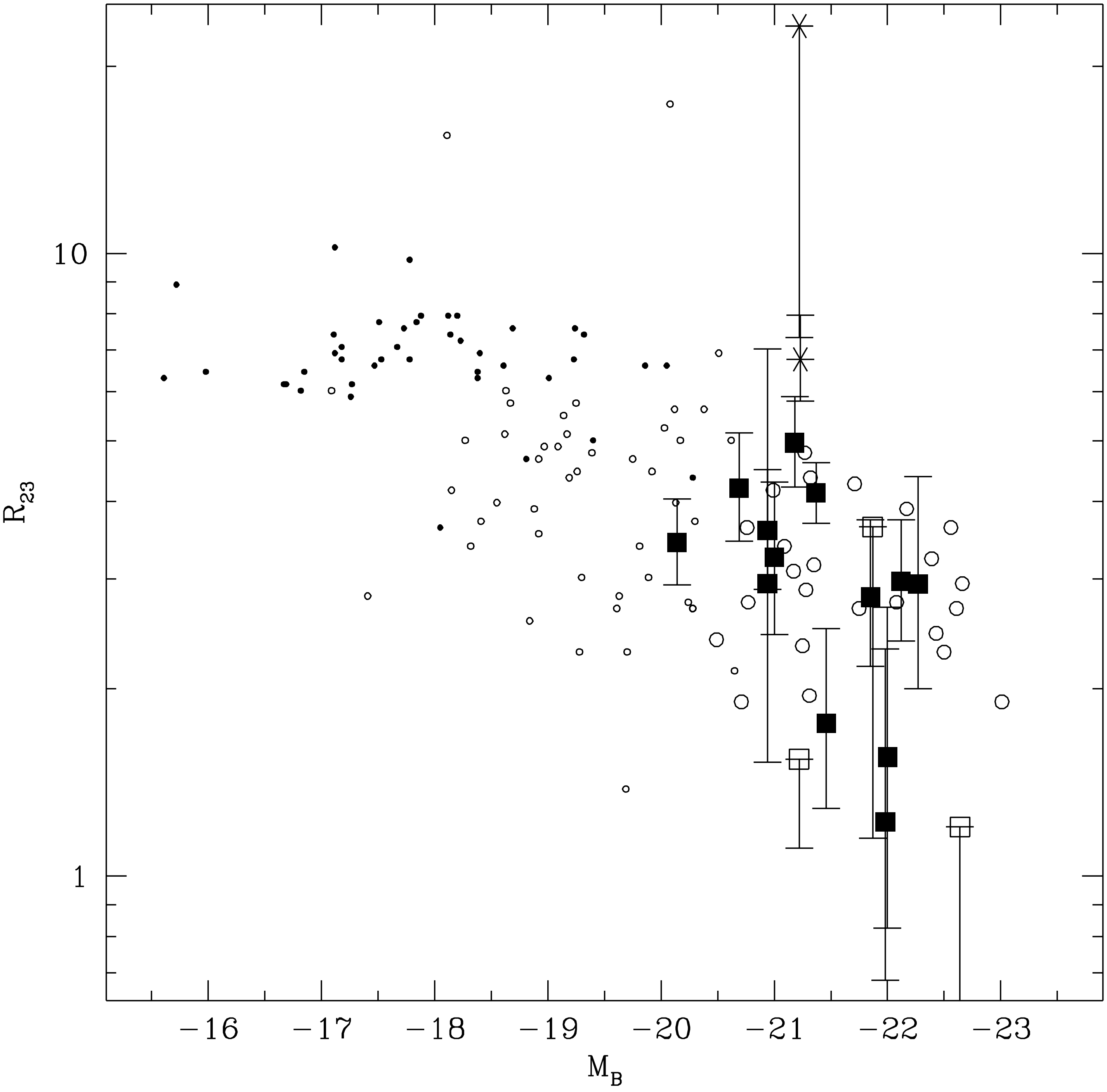

10
1
R_{23}
−16
−17
−18
−19
−20
−21
−22
−23
M_B